Probing Phase-Separation Behavior in Polymer-Blend Microparticles: Effects of Particle Size and Polymer Mobility

M. D. Barnes,* K. C. Ng,† K. Fukui, B. G. Sumpter, and D. W. Noid

Chemical and Analytical Sciences Division, Mail Stop 6142, Oak Ridge National Laboratory, Oak Ridge, Tennessee 37831

Received May 28, 1999; Revised Manuscript Received August 13, 1999

ABSTRACT: We describe a new method for probing phase separation of polymer-blend systems in spherical microparticles generated from microdroplets of dilute polymer solution. Two-dimensional optical diffraction—a technique sensitive to material inhomogeneity on a length scale of ≈30 nm—is used to probe phase-separation behavior of bulk-immiscible polymers in attoliter and femtoliter volumes. Under conditions of rapid solvent evaporation (≈2−10 ms) and relatively low polymer mobility, homogeneous composite particles can be formed using different polymers that ordinarily undergo phase separation in bulk preparations. We show that, for homogeneous particles, the refractive index (related to material dielectric constant) can be tuned by adjusting the relative weight fractions of polymers in the blend. Molecular dynamics simulations of polymer-blend microparticles are presented to illustrate at a molecular level effects of polymer interactions and boundary conditions on phase separation in polymer-blend nanoparticles. Finally, we show that polymer mobility affects phase-separation behavior in microparticles using mixtures of poly(vinyl alcohol)s with low molecular weight (high-mobility) poly(ethylene glycol) oligomers. For higher molecular weight polymers (>10 K), surface energy constraints inhibit phase separation, and the polymer-blend particles are observed to be homogeneous to within experimental resolution. Conversely, blends of low molecular weight PEG with PVA phase-separate on a time scale of several minutes to form heterogeneous composite particles.

Introduction

Recently, enormous commercial and scientific attention has been focused on multicomponent polymer systems as a means for producing new materials on the micron and nanometer scale with specifically tailored material, electrical, and optical properties.[1] Composite polymer particles, or polymer alloys, with specifically tailored properties could find many novel uses in such fields as electrooptic and luminescent devices,[2,3] conducting materials,[4] and hybrid inorganic−organic polymer alloys.[5] A significant barrier to producing many commercially and scientifically relevant homogeneous polymer blends,[6−9] however, is the problem of phase separation from bulk-immiscible components in solution that has been studied in detail by several different groups.[10−12] The route typically taken in trying to form homogeneous blends of immiscible polymers is to use compatibilizers to reduce interfacial tension. Recently, a number of different groups have examined phase separation in copolymer systems to achieve ordered meso- and microphase-separated structures with a rich variety of morphologies.[13,14] For solvent-cast composites, phase separation and related morphologies depend on the time scale for solvent evaporation relative to molecular organization.

Our interest is in using small droplets (≈5−10 μm diameter) of dilute mixed-polymer solution to form homogeneous polymer composites without compatibilizers as a possible route to new materials with tunable properties. The primary condition for suppression of phase separation in these systems is that solvent evaporation must occur on a time scale that is fast compared to self-organization times of the polymers. This implies time scales for particle drying on the order of a few milliseconds—a condition that can be satisfied with small droplets (≤10 μm), high vapor-pressure solvents, or modified droplet environment. We have shown recently that a microdroplet approach can be used to form homogeneous composites of codissolved bulk-immiscible polymers[15] using instrumentation developed in our laboratory for probing single fluorescent molecules in droplet streams.[16,17] In addition to a new route to forming nanoscale polymer composites, a microparticle format offers a new tool for studying multicomponent polymer-blend systems confined to femtoliter and attoliter volumes where high surface area-to-volume ratios play a significant role in phase-separation dynamics.

In this paper, we describe in some detail the basis of optical diffraction in spherical dielectric particles as a probe of material homogeneity in polymer composites and discuss limitations on the size dependence on the "visibility" of phase-separated domains in heterogeneous composite particles. We show how this measurement technique can be used to recover information on drying kinetics, interpolymer dynamics, molecular diffusion, and material properties such as dielectric constant. We also describe results of detailed molecular dynamics modeling that can be used to connect experimental observables with microscopic dynamics within the particle. Finally, we summarize important conclusions and discuss some possible future applications.

Experimental Section

Light scattering from micron-sized spherical dielectric droplets or particles[18] has been used for a number of years as a method of sizing[19−21] and analysis of various physical and chemical properties.[22,23] While various light scattering techniques from spherical droplets have been very well character-

† Permanent address: California State University, Fresno, Department of Chemistry, Fresno, CA 93740.

* To whom corresponce should be addressed.

10.1021/ma990846r CCC: $18.00
Published on Web 09/30/1999

ized for particle sizing and refractive index determination,[24−27] use of 1- and 2-dimensional angle-resolved elastic scattering has only very recently begun to be utilized as a tool for characterizing polymer systems.[15,28−31] The basis of the technique involves illumination of a dielectric sphere with a plane-polarized laser to produce a nonuniform electric field intensity distribution, or grating, within the particle that results from interference between refracted and totally internally reflected waves within the particle. The angular spacing between intensity maxima, as well as the intensity envelope, is a highly sensitive function of particle size and refractive index (both real and imaginary parts).

We have recently shown theoretically and experimentally[35] that two-dimensional optical diffraction is sensitive to material inhomogeneity on a length scale of ≈30 nm—a length scale comparable to radii of gyration for large molecular weight polymers. Qualitatively, phase separation within the particle results in a nonuniform refractive index which manifests itself as vertical distortion (or complete absence) of diffraction fringes. Quantitatively, material inhomogeneity is manifested in poor agreement with Mie theory calculations as well as subtle differences (as compared with homogeneous particles) in Fourier transforms of vertical fringes.[35] In our experimental configuration, far-field diffraction data were acquired using (*f*/1.5) collimating optics and a thermoelectrically cooled CCD camera (SpectraSource Instruments) digitized at 16 bits.[32] The transformation parameters connecting pixel number with scattering angle are established by means of an external calibration and used for high-precision Mie analysis of one-dimensional diffraction data.

For optical diffraction studies, individual particles were studied using droplet levitation techniques. Details of the apparatus and CCD calibration procedure are described in ref 32. The nominal scattering angle was 90° with respect to the direction of propagation of the vertically polarized HeNe laser, and the useable full plane angle (defined by the *f*/1.5 achromatic objective) was 35°. Details of the droplet generator used are described in ref 17. Aqueous solutions were handled by simply loading the Pyrex tip by vacuum aspiration and reinstalling into the generator. For the work done on codissolved polymers in tetrahydrofuran (THF), the entire droplet generator chamber and ballast reservoir were backfilled with THF, and the tip was loaded with the polymer solution of interest.

In the work reported here, we used a 60 Hz ac potential for particle levitation. Because of charge-to-mass instabilities, particles having a diameter smaller than about 2 μm are not trapped effectively at 60 Hz. This limitation can be overcome by using higher frequencies at the expense of additional experimental complexity.[33] A more serious issue is the limited information content in the data for particles smaller than about 2 μm. The plane angle subtended by the collection objective imposes a lower bound on the size range of particles since the angular frequency of intensity maxima (number of fringes per unit angle) decreases with particle size. Also, the fringes become broader and the contrast (depth of modulation) becomes poorer. For particles smaller than ≈1.5 μm in diameter (more precisely, for particles with a size parameter $d/\lambda < 2$, where λ is the probe wavelength), at most only one diffraction fringe is present in a scattering window of 35°, which limits the ability to analyze the data unambiguously.

Thus, we estimate that diffraction from particles smaller than about 1.5 μm would be difficult to analyze quantitatively in our current experimental configuration. In addition, the integrated scattered light intensity decreases approximately as the square of the diameter in this size range; compensation for this effect by increasing laser power often adds the complication of photon pressure,[33] resulting in position fluctuations that further exacerbate the problem.

Results

Figure 1 shows one-dimensional diffraction data for a poly(ethylene glycol) particle (10K average molecular weight) produced from aqueous solution and Mie theory

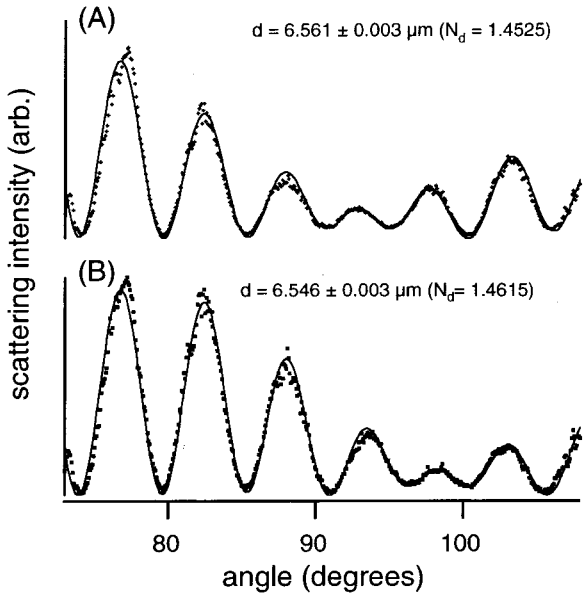

Figure 1. One-dimensional (row) slices of measured two-dimensional diffraction patterns (points) and Mie theory fits (solid curves) from a levitated poly(ethylene glycol) particle at two different times. The size and refractive index differences between the two exposures are 15 nm and 0.009, respectively, and reflect a small loss of water by the particle during the measurement sequence.

matches to the data. The upper and lower traces (A and B, respectively) are two exposures at different times from the same particle and illustrate the sensitivity of the technique to both particle size and refractive index. The differences in particle size (15 nm) and refractive index (+0.009) reflect the loss of a small amount of residual water in the 5 min time interval between exposures. The points are measured scattering intensities as a function of laboratory angle, and the smooth curves are Mie theory matches to the data optimized with respect to particle size and both real and imaginary parts of the refractive index. Note that the Mie analysis is not a "fit" to the data in the sense of a nonlinear least-squares optimization of parameters or coefficients associated with some predefined function. Three independent factors define the scattering pattern—size, Re(*n*), and Im(*n*)—and are systematically varied to find the best possible match to the experimental data by locating the minimum in a 4-dimensional error function.

Figure 2 shows a family of 2-D slices (Re(*n*) varied and Im(*n*) fixed) of a typical error surface obtained from data acquired for a PEG particle. From exhaustive analysis of these error surfaces from many different sized particles, we find absolute size uncertainties to be between 2 and 5 nm and the uncertainty in Re(*n*) to be between 10^{-3} and 5×10^{-4}. For materials with a low molar absorptivity (typical of most liquids), Im(*n*) is correspondingly small—on the order of 10^{-5}−10^{-7}. At these values, there is very little (if any) effect on the match to data by varying Im(*n*). For many polymers (poly(vinyl chloride)s, for example) however, this is not the case, and Im(*n*) can be as large as 10^{-3}. At this order of magnitude, Im(*n*) does influence the Mie analysis of the data.

A key issue in forming homogeneous composites from codissolved bulk-immiscible polymers from solution is that the droplet evaporation rate must be fast compared with the polymer self-organization time scale. Since the time scale for solvent evaporation is proportional to

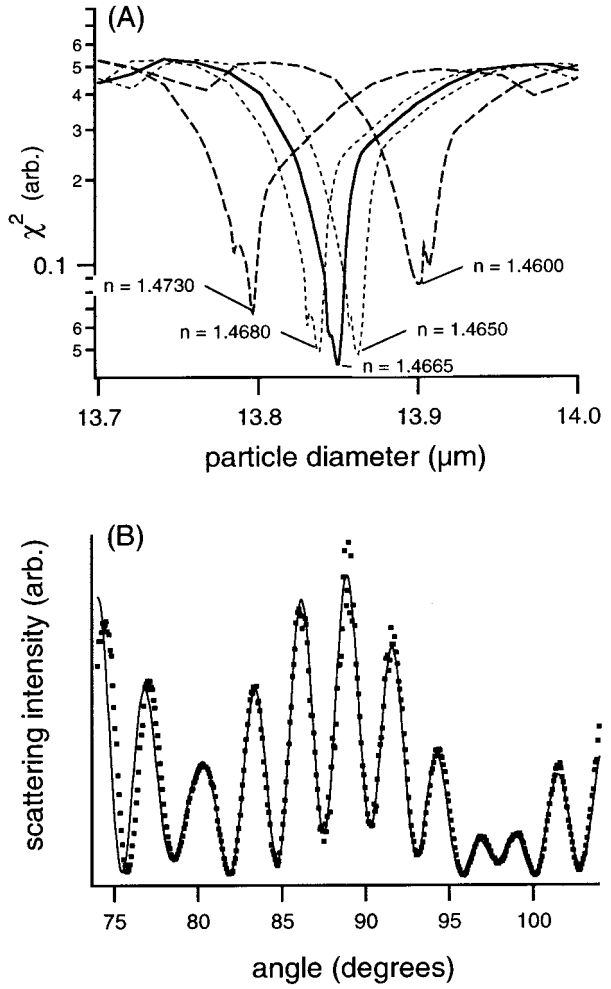

Figure 2. Two-dimensional slices of 4-dimensional error surface (varying Re(n)) for Mie theory match to diffraction from PEG particle (Im(n) fixed). The lower trace shows the best match to the experimental scattering data.

$1/(r^{3/2})$ where r is the droplet radius, the most straightforward way to satisfy this condition is to make droplets smaller.[16] Alternatively, one can modify the atmosphere around the droplet (temperature, different bath gases, etc.) to accelerate particle drying.[17] As part of our effort in developing single-molecule isolation and manipulation methodologies in droplet streams, we have been able to produce (water) droplets as small as 2−3 μm in diameter with ≈1% size dispersity.[16]

Figure 3 shows an experimental characterization of evaporation of a pure water droplet on a millisecond time scale using a high-speed frame transfer CCD camera. Angular scattering data were acquired at successive 1 ms intervals during the 5 ms transit of the droplet through the laser beam. The deviation of the third and fifth points from the model most likely originate from a "phase aliasing" due to particle motion induced from photon pressure. For evaporation rates similar to that shown in Figure 3, approximately 95% of the initial droplet volume is lost due to evaporation in about 5 ms. On this time scale, diffusional motion of the polymer center of mass is negligible.[34]

We have recently shown that the presence of phase-separated structures in polymer-blend microparticles can be indicated qualitatively by a distortion in the two-dimensional diffraction pattern.[15] The origin of fringe distortion from a multiphase composite particle can be

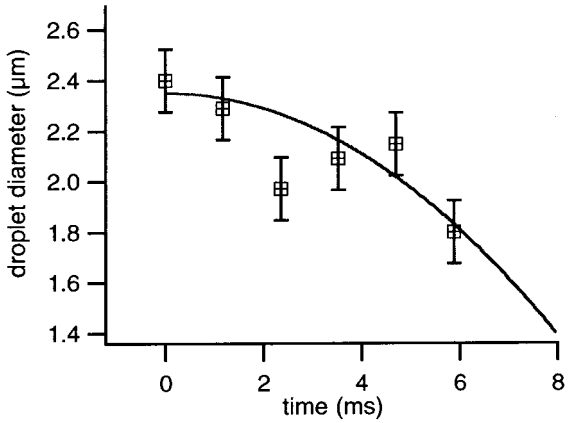

Figure 3. Characterization of rapid evaporation from a 2.4 μm diameter (pure) water droplet using angular scattering and a high-speed frame transfer CCD camera. Since the CCD pixel transformation parameters were not precisely defined in these experiments, the errors are estimated to be on the order of the diffraction limit.

understood as a result of refraction at the boundary between domains of different polymers, which typically exhibit large differences in refractive index. Phase-separated subdomains within the particle (regions within the particle that are rich in one or the other blend component) introduce optical phase shifts and refraction resulting in a "randomization" (distortion) in the internal electric field intensity distribution that is manifested as a distortion in the far-field diffraction pattern. Of particular interest is the minimum size of such domains to result in a measurable (quantifiable) distortion. Recently, we have investigated in detail effects of phase-separated domain size and number density both experimentally and theoretically using polymer/ceramic heterogeneous composite particles.[35] These studies confirm sensitivity of this technique to material inhomogeneity on a length scale of about 30 nm. The "visibility" of phase-separated domains is related to the total scattering cross section which scales such as d^6/λ^4, where d is the domain size and λ is the probe wavelength. For large molecular weight polymers, this length scale is comparable to radii of gyration, thus providing a method of looking "within" a composite particle and probing material homogeneity on a molecular scale.

Another important aspect of our approach is the ability to obtain very precise information on the refractive index. This provides a way of characterizing material properties that would not be possible with conventional microscopy techniques. One can, for example, directly measure kinetics of particle drying by monitoring the change in refractive index as the solvent evaporates. In general, we find that the particle drying kinetics have two distinct solvent evaporation regimes. When the droplet is first ejected, the size decreases rapidly with most of the solvent evaporation taking place within the first 10−100 ms. This is followed by a much slower ("wet particle") evaporation regime where the particle continues to lose solvent on a time scale of several minutes (dependent on size). Interestingly, in the slow-evaporation regime, we generally observe that the volume change expected from solvent loss (assuming an ideal solution) is *not* accompanied by the expected corresponding change in particle size.

Homogeneous and Phase-Separated Composite Microparticles. As a proof-of-concept test case, we examined two bulk-immiscible polymers (polystyrene

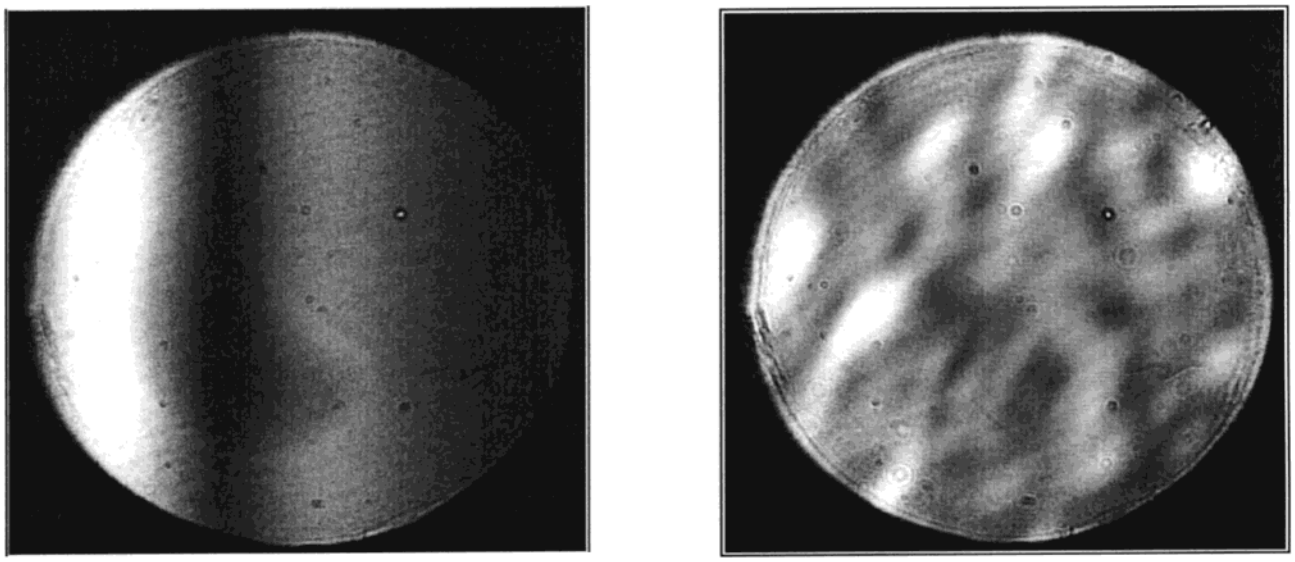

Figure 4. Two-dimensional diffraction data from 50:50 w/w PVC/PS blend particles produced from an 8 μm diameter droplet (left) and a 35 μm diameter droplet (right).

and poly(vinyl chloride)) that are both soluble in THF.[15] As a verification, we have examined PVC/PS solvent-cast thin films using phase-contrast microscopy, and clear evidence of phase separation (solid-phase emulsions) were observed. We have not characterized evaporation rates of pure THF droplets but estimate on the basis of vapor pressure differences relative to water that evaporation is roughly a factor of 5 more rapid (for a given droplet size). To provide some kind of scale, a water droplet with an initial diameter of 10 μm will evaporate to $\approx$1 μm diameter in about 5 ms in a dry argon atmosphere.[17]

Figure 4 shows examples of PVC/PS particles formed from an (A) 8 μm diameter droplet and (B) a 35 μm diameter droplet of dilute ($\approx$1% total polymer weight fraction) PVC/PS/THF solution. The size threshold (for this system) for producing homogeneous particles is about 10 μm. For larger droplets that have correspondingly longer drying times, we observed that the particles were inhomogeneous. There is compelling evidence for material homogeneity at a molecular length scale for the particle represented in Figure 4a: fringe uniformity, quantitative agreement with Mie calculations, and a refractive index (related to material dielectric constant) that is intermediate between the two pure materials. The radius of gyration of the polystyrene (500K MW) is approximately 25 nm, which is comparable to the domain size resolution of the technique. It should be noted that for heterogeneous particles, while the diffraction fringes are highly distorted, there remains some definite two-dimensional structure. This implies some uniformity and order of phase-separated subdomains; however, inversion of this type of data to extract such information is not trivial. This problem is currently under investigation. (See also ref 30.)

Figure 5 shows time-resolved results of particle size and refractive index for a 2.4 μm PVC/PS (50:50 w/w) blend particle. Note that the particle continues to "dry" on a time scale of several minutes but remains homogeneous throughout the measurement sequence. The nominal index of pure THF is 1.41, and the measured (steady state) final index of the particle is 1.527. These limiting values suggest that, for the first data point in Figure 5, the particle is 22 vol % THF. Assuming that

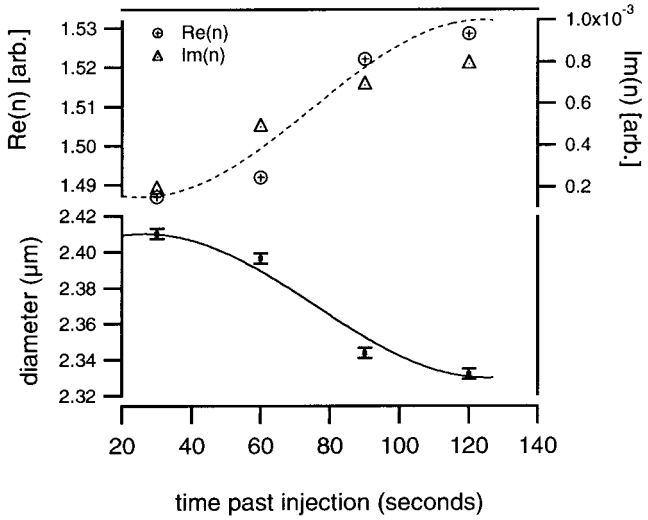

Figure 5. Particle size and refractive index for a PVC/PS composite particle (50:50 w/w) as a function of time past injection. The solid/dashed curves shown are trial best-fit functions combining a $r^{-3/2}$ dependence with an e^{-r} (or $1 - e^{-r}$) asymptotic behavior.

the last data point represents a fully dry particle (in good agreement with estimates based on refractive indices for pure PS and PVC), one would have expected a 60% *decrease* in particle size accompanying the loss of residual THF. This is clearly not observed, indicating that the particle has formed a fairly rigid matrix that compresses only slightly ($\approx$3%) during the exposure sequence.

The data shown in Figure 5 also illustrate the "tunable" nature of a material property in PVC/PS composite particles—namely the dielectric constant manifested in the refractive index. Both Re(n) and Im(n) for the polymer-blend microparticles are intermediate between the values determined for pure single-component particles (PVC: Re(n) = 1.4780, Im(n) = 10^{-3}; PS: Re(n) = 1.5908, Im(n) = 2×10^{-5}) and can be controlled by adjusting the weight fractions of polymers. Interestingly, the measured refractive index for composite particles are very close to estimates obtained from a simple mass-weighted average of the two species.

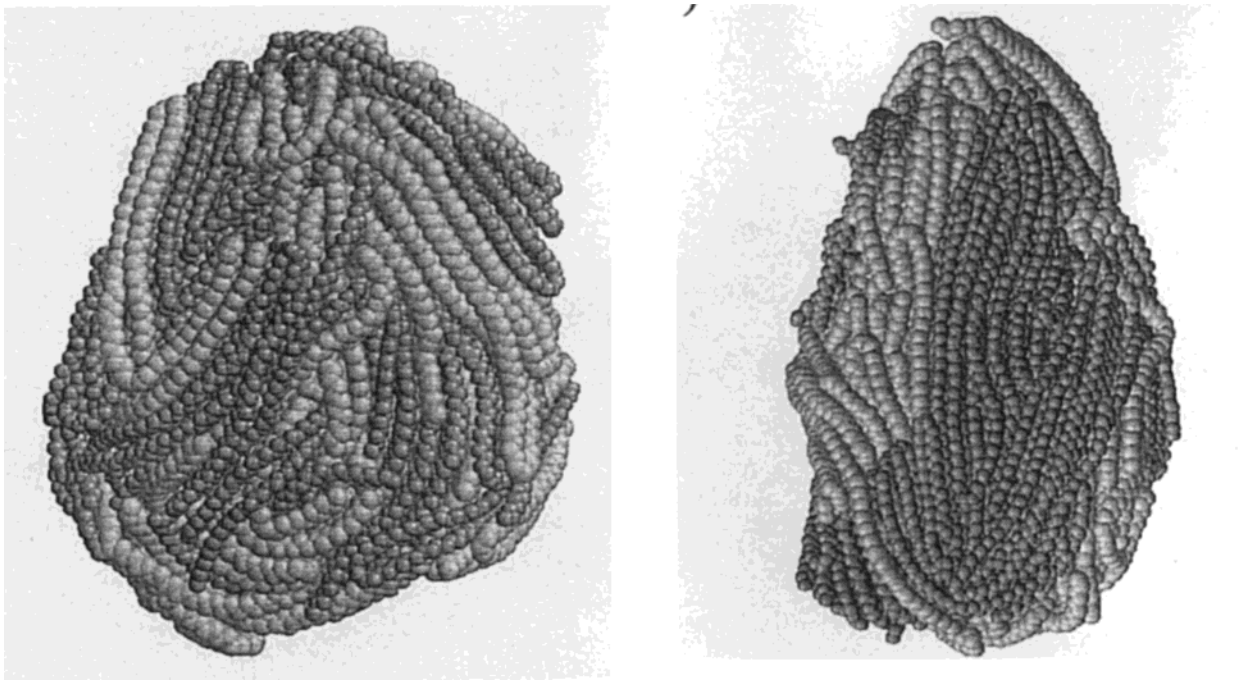

Figure 6. Calculated structures for homogeneous (left) and phase-separated (right) 10 nm polymer blend particles.

In addition to our experimental effort, we have also investigated this problem using molecular dynamics simulation tools in order to develop some insight into the structure and properties of polymer-blend particles. Using classical molecular dynamics techniques, we have examined polymer nanoparticles of varying size (up to 300 000 atoms), chain lengths (between 50 and 200 monomers), and intermolecular interaction energy allowing the systematic study of size-dependent physical properties and time dependence of segregation/equilibration of these particles.

Figure 6 shows molecular dynamics simulations of a stable polymer-blend particle (10 nm diameter) composed of immiscible components.[36] The leftmost particle remains homogeneous throughout a broad temperature range. For phase separation to occur (right), an enormous amount of thermal energy must be supplied in order to overcome the surface energy barrier. This result agrees qualitatively with the observation that homogeneous blends of bulk-immiscible polymers can be formed in spherical microparticles. The composite particle was calculated to have a *single* melting temperature of 190 K and glass transition temperature of 90 K which is different than either of the polymer components (T_m = 218 K, T_g = 111 K for light and T_m = 162 K, T_g = 81 K for dark). The segregated particle has two melting points and glass transition temperatures that correspond to within 10 K of the individual components.

Formation of homogeneous polymer-blend composites from bulk-immiscible codissolved components using droplet techniques has two requirements. First, solvent evaporation must occur on a relatively short time scale compared to polymer translational diffusion. Second, the polymer mobility must be low enough so that, once the solvent has evaporated, the polymers cannot overcome the surface energy barrier and phase-separate. We have shown definitively the effects of droplet size and solvent evaporation, and the second requirement is almost always satisfied even for modest molecular weight polymers. To explore effects of polymer mobility in more detail, we looked at composite particles of PEG oligomers (MW 200, 400, 1000, and 3400) with medium molecular weight (14K) atactic poly(vinyl alcohol) (PVA). This system allows us to systematically examine the phase separation behavior where one component (PEG) has substantially different viscosities (specified as 4.3, 7.3, and 90 cSt at room temperature for PEG [200], PEG [400], and PEG [3400], respectively).

We observed that the higher molecular weight PEG polymer-blend particles are homogeneous as determined from bright-field microscopy, optical diffraction, and fluorescence imaging. Blend particles prepared with the 200 molecular weight PEG were observed to form sphere-within-a-sphere particles with a PVA central core. Figure 7 shows diffraction data acquired from particles at successive 10 min intervals from a 10 μm diameter PEG[200]/PVA[14K] (80:20 w/w) particle. As shown in the first frame, the particle is initially homogeneous. The second and third frames indicate that the composite particle undergoes phase separation into an inhomogeneous particle as evidenced by the fringe distortion. Interestingly, the structure in the 2D diffraction data for this system is much different than those observed for large phase-separated PVC/PS particles that presumably coalesce into submicron spheroidal domains.

On the basis of fluorescence and phase-contrast imaging data, PEG[200]/PVA[14K] particles form spherically symmetric (sphere-within-a-sphere) heterogeneous structures, which should also produce well-defined diffraction fringes.[37−39] Our interpretation of these data is that diffusional motion of the PVA core in the PEG host particle, combined with rotational diffusion of the particle, breaks the spherical symmetry and thereby introduces distortion in the diffraction pattern. This observation is entirely consistent with our model of polymer-composite formation where heterogeneous particles may be formed provided that the mobility of one of the polymers is low enough to overcome the surface energy barrier. From the 20 min time scale for phase

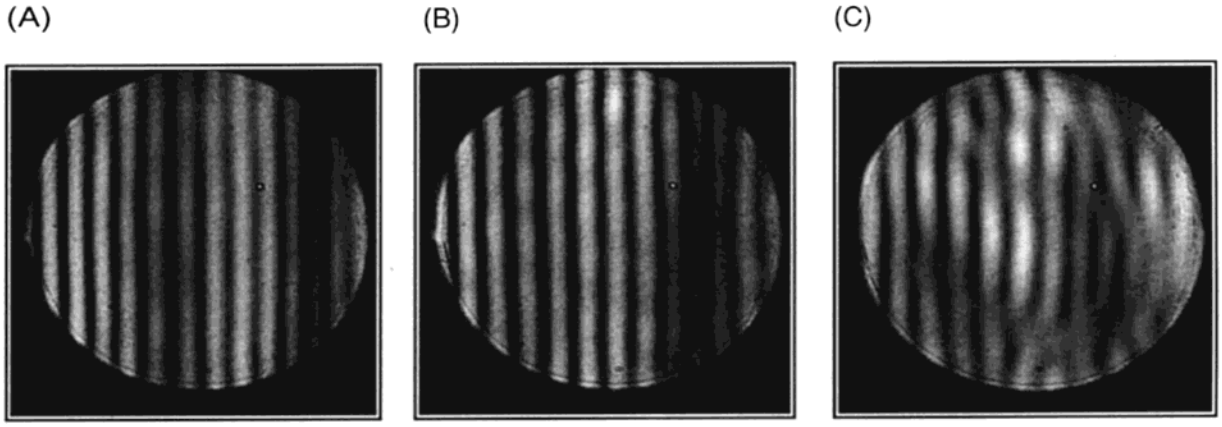

Figure 7. Two-dimensional diffraction data acquired at successive 10 min intervals from a 10 μm diameter (nom.) PEG[200]/PVA[14K] (80:20 w/w) particle.

separation in the low molecular weight PEG system, we estimate a diffusion coefficient of 10^{-10} cm^2/s, which is consistent with recent molecular modeling results. For a diffusion coefficient, D, of 10^{-10} cm^2/s and 1200 s time scale, the average diffusion distance $r = (6Dt)^{1/2} = 8.5$ μm, which is comparable to the particle diameter. Composite particles formed from the higher molecular weight PEG (>1000) form homogeneous composite particles with PVA.

Summary and Conclusions

The combination of experimental evidence and computational modeling shows conclusively that stable, homogeneously blended (bulk-immiscible) mixed-polymer composites can be formed in a single microparticle of variable size. To our knowledge, this represents a new method for suppressing phase separation in polymer-blend systems without compatibilizers that allows formation of polymer composite micro- and nanoparticles with tunable properties such as dielectric constant. Conditions of rapid solvent evaporation (e.g., small (<10 μm) droplets or high-vapor-pressure solvents) and low polymer mobility must be satisfied in order to form homogeneous particles. In addition, we showed that polymer diffusion coefficients in the microparticle could be estimated to an order of magnitude by time-resolved diffraction measurements. While this work was obviously focused on polymer-blend systems, it should be pointed out that the technique is easily adaptable to making particles of small organic and inorganic (and hybrid composites) as well. A wide range of electronic, optical, physical, and mechanical properties of single-component and multicomponent polymer nanoparticles remain to be explored.

Acknowledgment. This research was sponsored by the U.S. Department of Energy, Office of Basic Energy Sciences (Divisions of Chemical Sciences and Materials Science), under Contract DE-AC05-96OR22464 with Oak Ridge National Laboratory and Laboratory-Directed Research and Development Seed Money Fund managed by Lockheed Martin Energy Research Corporation. K. C. Ng acknowledges support from the ORNL Faculty Research Participation Program. K. Fukui acknowledges support from the ORNL Postdoctoral Research Program.

References and Notes

(1) Binder, K. *J. Non-Equilib. Thermodyn.* **1998**, *23*, 1−44 and references therein.
(2) Jenekhe, S. A.; Zhang, X. J.; Chen, X. L.; Choong, V. E.; Gao, Y. L.; Hsieh, B. R. *Chem. Mater.* **1997**, *9*, 409−413.
(3) Tarkka, R. M.; Zhang, X. J.; Jenekhe, S. A. *J. Am. Chem. Soc.* **1996**, *118*, 9438−9439.
(4) Croce, F.; Appetecchi, G. B.; Persi, L.; Scrosati, B. *Nature* **1998**, *394*, 456−458.
(5) Schwerzel, R. E.; Spahr, K. B.; Kurmer, J. P.; Wood, V. E.; Jenkins, J. A. *J. Phys. Chem. A* **1998**, *102*, 5622−5626.
(6) Xanthos, M. *Polym. Eng. Sci.* **1988**, *28*, 1392−1416.
(7) Koning, C.; van Duin, M.; Pagnoulle, C.; Jerome, R. *Prog. Polym. Sci.* **1998**, *23*, 707−757.
(8) Paul, D. R. In *Polymer Blends*; Paul, D. R., Newman, S., Eds.; Academic Press: New York, 1978; Vol. II, pp 35−62.
(9) Utracki, L. A. *Polymer Alloys and Blends: Thermodynamics and Rheology*; Oxford University Press: New York, 1990.
(10) Sung, L.; Karim, A.; Douglas, J. F.; Han, C. C. *Phys. Rev. Lett.* **1996**, *76*, 4368−4371.
(11) Yu, J. W.; Douglas, J. F.; Hobbie, E. K.; Kim, S.; Han, C. C. *Phys. Rev. Lett.* **1997**, *78*, 2664−2667.
(12) Marcus, A. H.; Hussey, D. M.; Diachun, N. A.; Fayer, M. D. *J. Chem. Phys.* **1996**, *103*, 8189−8200.
(13) Jenekhe, S. A.; Chen, X. L. *Science* **1998**, *279*, 1903−1906. Jenekhe, S. A.; Chen, X. L. *Science* **1999**, *283*, 372−375.
(14) Bates, F. S.; Fredickson, G. H. *Phys. Today* **1999**, *52*, 32−38 and references therein.
(15) Barnes, M. D.; Kung, C.-Y.; Fukui, K.; Sumpter, B. G.; Noid, D. W.; Otaigbe, J. U. *Opt. Lett.* **1999**, *24*, 121−123.
(16) Kung, C.-Y.; Barnes, M. D.; Lermer, N.; Whitten, W. B.; Ramsey, J. M. *Anal. Chem.* **1998**, *70*, 658−661.
(17) Kung, C.-Y.; Barnes, M. D.; Lermer, N.; Whitten, W. B.; Ramsey, J. M. *Appl. Opt.* **1999**, *38*, 1481−1487.
(18) We use the word "droplet" to denote liquid phase and "particle" to denote a solid (dry) phase.
(19) Chang, R.; Davis, E. J. *J. Colloid Interface Sci.* **1976**, *54*, 352−357.
(20) Davis, E. J.; Ray, A. K. *J. Colloid Interface Sci.* **1980**, *75*, 566−570.
(21) Ray, A. K.; Souyri, A.; Davis, E. J.; Allen, T. M. *Appl. Opt.* **1991**, *30*, 3974−3981.
(22) Widmann, J. F.; Aardahl, C. L.; Davis, E. *J. Am. Lab.* **1996**, *28*, 35−37.
(23) See also, the review by: Davis, E. J. *Aerosol Sci. Technol.* **1997**, *26*, 212−254.
(24) Chylek, P.; Ramaswamy, V.; Ashkin, A.; Dziedzic, J. M. *Appl. Opt.* **1983**, *22*, 2302−2311.
(25) Van de Hulst, H. C.; Wang, R. T. *Appl. Opt.* **1991**, *30*, 4755−4761.
(26) Konig, G.; Anders, K.; Frohn, A. *J. Aerosol Sci.* **1986**, *17*, 157−162.
(27) Glover, A. R.; Skippon, S. M.; Boyle, R. D. *Appl. Opt.* **1995**, *34*, 8409−8422.
(28) Widmann, J. F.; Davis, E. J. *Colloid Polym. Sci.* **1996**, *274*, 525−531.
(29) Kaiser, T.; Lange, S.; Schweiger, G. *Appl. Opt.* **1994**, *33*, 7789−7797.

(30) Holler, S.; Pan, Y.; Chang, R. K.; Bottiger, J. R.; Hill, S. C.; Hillis, D. B. *Opt. Lett.* **1998**, *23*, 1489−1491.
(31) Widmann, J. F.; Aardahl, C. L.; Johnson, T. J.; Davis, E. J. *J. Colloid Interface Sci.* **1998**, *199*, 197−205.
(32) Barnes, M. D.; Lermer, N.; Whitten, W. B.; Ramsey, J. M. *Rev. Sci. Instrum.* **1997**, *68*, 2287−2291.
(33) Lermer, N.; Barnes, M. D.; Kung, C.-Y.; Whitten, W. B.; Ramsey, J. M. *Anal. Chem.* **1997**, *69*, 2115−2121.
(34) For a polymer molecule with a modest molecular weight of say, 10^4, the diffusion coefficient is $\approx 10^{-9}$ cm^2/s in solution.
(35) Ford, J. V.; Sumpter, B. G.; Noid, D. W.; Barnes, M. D.; Hill, S. C.; Hillis, D. B. Domain size effects in 2-dimensional optical diffraction from polymer microparticles doped with nanometer-sized inclusions, submitted to *J. Phys. Chem. B*.
(36) Fukui, K.; Sumpter, B. G.; Otaigbe, J. U.; Barnes, M. D.; Noid, D. W. *Macromol. Theory Simul.* **1999**, *8*, 38−45.
(37) Lock, J. A. *Appl. Opt.* **1990**, *29*, 3180−3187.
(38) Ray, A. K.; Devakottai, B.; Souyri, A.; Huckaby, J. L. *Langmuir* **1991**, *7*, 525−531.
(39) Hightower, R. L.; Richardson, C. B.; Lin, H.-B.; Eversole, J. D.; Campillo, A. *J. Opt. Lett.* **1988**, *13*, 946−948.

MA990846R